

**Mechanistic investigation of benzene esterification by  $K_2CO_3/TiO_2$   
The catalytic role of the multifunctional interface**

Meeprasert, Jittima; Li, Guanna; Pidko, Evgeny A.

**DOI**

[10.1039/d1cc02513a](https://doi.org/10.1039/d1cc02513a)

**Publication date**

2021

**Document Version**

Final published version

**Published in**

Chemical Communications

**Citation (APA)**

Meeprasert, J., Li, G., & Pidko, E. A. (2021). Mechanistic investigation of benzene esterification by  $K_2CO_3/TiO_2$ : The catalytic role of the multifunctional interface. *Chemical Communications*, 57(64), 7890-7893. <https://doi.org/10.1039/d1cc02513a>

**Important note**

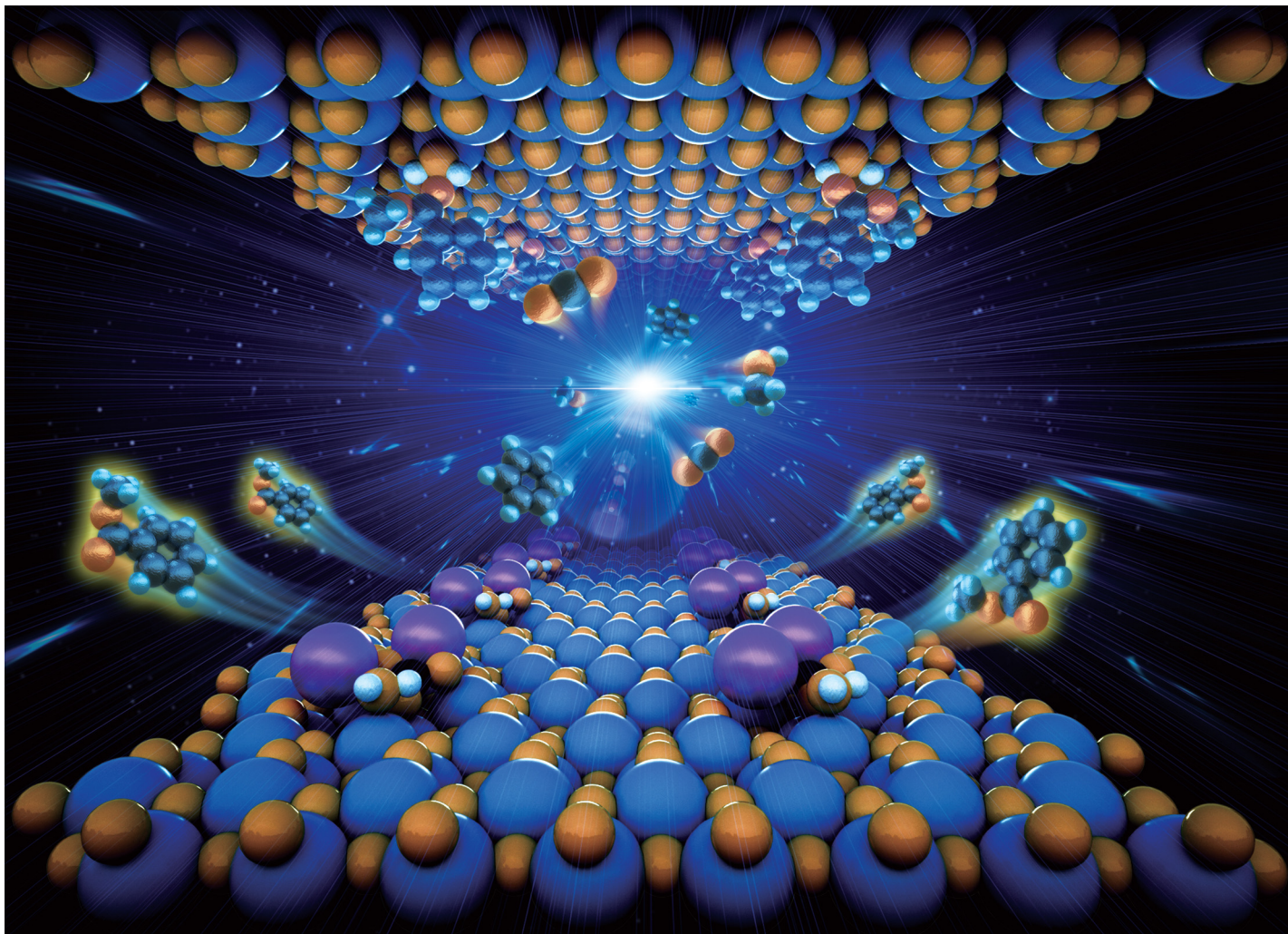
To cite this publication, please use the final published version (if applicable).  
Please check the document version above.

**Copyright**

Other than for strictly personal use, it is not permitted to download, forward or distribute the text or part of it, without the consent of the author(s) and/or copyright holder(s), unless the work is under an open content license such as Creative Commons.

**Takedown policy**

Please contact us and provide details if you believe this document breaches copyrights.  
We will remove access to the work immediately and investigate your claim.



Showcasing research from Professor Pidko's laboratory, Inorganic Systems Engineering, Department of Chemical Engineering, Delft University of Technology, Delft, The Netherlands.

Mechanistic investigation of benzene esterification by  $\text{K}_2\text{CO}_3/\text{TiO}_2$ : the catalytic role of the multifunctional interface

The detailed reaction mechanism of benzene carboxylation with  $\text{CO}_2$  and subsequent methylation by  $\text{CH}_3\text{OH}$  was investigated over the catalysts of  $\text{TiO}_2$  and  $\text{K}_2\text{CO}_3/\text{TiO}_2$ . The multicomponent and multifunctional  $\text{K}_2\text{CO}_3\text{-TiO}_2$  interface facilitates product desorption and interfacial active sites regeneration.

As featured in:



See Guanna Li, Evgeny A. Pidko *et al.*, *Chem. Commun.*, 2021, **57**, 7890.


 Cite this: *Chem. Commun.*, 2021, 57, 7890

 Received 18th May 2021,  
Accepted 16th July 2021

DOI: 10.1039/d1cc02513a

rsc.li/chemcomm

## Mechanistic investigation of benzene esterification by $K_2CO_3/TiO_2$ : the catalytic role of the multifunctional interface†

 Jittima Meeprasert,<sup>a</sup> Guanna Li<sup>\*,bc</sup> and Evgeny A. Pidko<sup>\*,a</sup>

**Potassium carbonate dispersed over a defective  $TiO_2$  support ( $K_2CO_3/TiO_2$ ) is an efficient catalyst for benzene esterification with  $CO_2$  and  $CH_3OH$ . Density functional theory calculations reveal that this unique catalytic reactivity originates from the cooperation of the  $Ti^{3+}/K^+$  surface sites. The  $K_2CO_3$  promotor steers the stabilization of surface intermediates thus preventing catalyst deactivation.**

$CO_2$  conversion into valuable chemicals has received much attention due to the environmental concerns associated with the growing atmospheric concentrations of greenhouse gases. Many efforts have been invested to develop the economic carbon-neutral system by recycling the carbon resource of  $CO_2$  from industrial emission to the production of chemicals.<sup>1–3</sup> The carboxylation of aromatics by  $CO_2$  is one of the attractive routes for the valorization of  $CO_2$ , because the produced aromatic carboxylic acids and their derivatives can serve as important chemical feedstocks.<sup>4,5</sup> Conventionally, such a carboxylation coupling reaction is carried out in the presence of a strong base or Lewis acid such as  $NaH$ ,<sup>6</sup>  $AlCl_3$ ,<sup>4</sup> and  $AlBr_3$ .<sup>7</sup> The strong base is needed to cleave the C–H bond of arene to form a nucleophilic carbon atom which can further interact with the weak  $CO_2$  electrophile. The role of the Lewis acid is to activate the  $CO_2$  molecule before the arene C–H bond carboxylation.<sup>8</sup> However, both these strategies usually provide rather low yields of the target products due to the low electrophilicity of  $CO_2$  and side reactions caused by excessive reactivity of the mediators.<sup>7,8</sup> Therefore, the development of alternative catalytic procedures avoiding the usage of strong base or acid is highly desired but also represents one of the great challenges for this reaction.

Recently, Kanan *et al.* reported that alkali carbonates ( $K_2CO_3$  and  $Cs_2CO_3$ ) finely dispersed over a  $TiO_2$  support can promote the two-step cycle of benzene esterification with  $CO_2$  and  $CH_3OH$  to produce methyl benzoate with both high yield (80%) and high selectivity (100%) in the absence of stoichiometric additives.<sup>9</sup> It is important to note that bare  $TiO_2$  can also promote the first step of benzene C–H bond carboxylation, however, the catalyst became deactivated after just one catalyst recycling. In contrast, no carboxylation products were observed when  $K_2CO_3$  or  $Cs_2CO_3$  powders as the only catalyst component were used. Thus, it was hypothesized that dispersing alkali carbonate over  $TiO_2$  would engender catalytic carboxylation activity towards hydrocarbon substrates because of the disruption of the bulk alkali carbonate structure. However, the mechanistic aspects of this system, such as the nature of the active site, initiation of the reaction and the exact role of the different catalyst components, remained moot.<sup>8</sup> This inspired us to carry out a comprehensive mechanistic study of benzene carboxylation with  $CO_2$  and subsequent reaction with  $CH_3OH$  over the  $K_2CO_3/TiO_2$  catalyst by periodic density functional theory (DFT) calculations. Our main objective was to identify the role and function of each catalyst component and to propose the origin of the deactivation of bare  $TiO_2$  catalyst.

In this work, all calculations were performed using the Vienna *Ab Initio* Simulation Package (VASP) 5.3.5.<sup>10,11</sup> DFT calculations were carried out using PBE functional based on the generalized gradient approximation (GGA).<sup>12</sup> Grimme's DFT-D3 method with Becke-Jonson damping was used to account for the dispersion interactions.<sup>13</sup> The DFT+U method was applied to the 3d orbitals of Ti to correct the on-site Coulomb interactions. The U value used in this work is 4.2 eV.<sup>14</sup> The energy cutoff and convergence criteria for the electronic and ionic loops were 400 eV,  $10^{-5}$  eV, and  $0.05 \text{ eV } \text{Å}^{-1}$ , respectively. Transition states were determined by the nudged-elastic band method with the improved tangent estimate (CI-NEB) and subsequent frequency analysis. The model of  $K_2CO_3/TiO_2$  catalyst was built following the experimental evidence of the very fine dispersion of  $K_2CO_3$  on the surface of  $TiO_2$ .<sup>9</sup>

<sup>a</sup> Inorganic Systems Engineering, Department of Chemical Engineering, Delft University of Technology, The Netherlands. E-mail: e.a.pidko@tudelft.nl

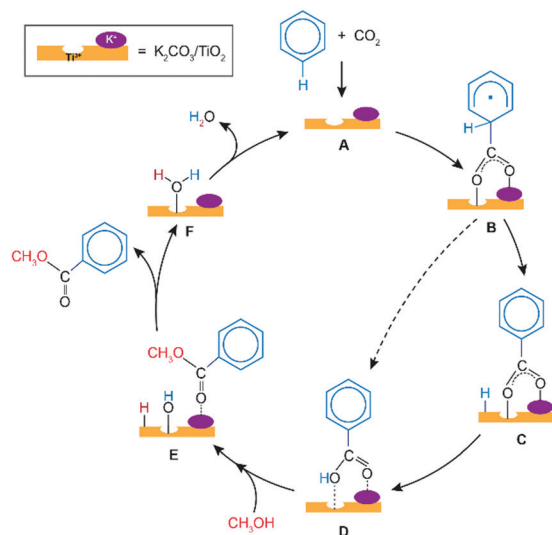
<sup>b</sup> Biobased Chemistry and Technology, Wageningen University & Research, The Netherlands. E-mail: guanna.li@wur.nl

<sup>c</sup> Laboratory of Organic Chemistry, Wageningen University & Research, The Netherlands

† Electronic supplementary information (ESI) available. See DOI: 10.1039/d1cc02513a







**Scheme 1** Proposed mechanism of benzene esterification with  $\text{CO}_2$  and  $\text{CH}_3\text{OH}$  on  $\text{K}_2\text{CO}_3/\text{TiO}_2$  catalyst. The  $\text{A} + \text{CO}_2 + \text{C}_6\text{H}_6 \rightarrow \text{D}$  conversion involves the carboxylation of benzene with  $\text{CO}_2$  via the one-step direct (dashed) or stepwise indirect (solid path) mechanisms to yield the adsorbed benzoic acid. The latter is methylated with  $\text{CH}_3\text{OH}$  ( $\text{D} + \text{CH}_3\text{OH} \rightarrow \text{F} + \text{C}_6\text{H}_5\text{COOCH}_3$ ) to yield methyl benzoate product and the adsorbed water. Subsequent desorption of  $\text{H}_2\text{O}$  by-product ( $\text{F} \rightarrow \text{A} + \text{H}_2\text{O}$ ) regenerates the catalytic surface ensemble.

Fig. S1 in the ESI† shows the catalyst model featuring the  $\text{K}_2\text{CO}_3$  species deposited on the defective anatase  $\text{TiO}_2(101)$  surface. We hypothesized that the interface of coordination-unsaturated surface Ti site ( $\text{Ti}^{3+}$ ) together with the adjacent  $\text{K}_2\text{CO}_3$  cluster form the

reactive ensemble because neither the bulk crystalline  $\text{K}_2\text{CO}_3$  nor the pristine  $\text{TiO}_2$  surface are active.<sup>9,15</sup>

Scheme 1 presents a proposed reaction mechanism for the esterification of benzene with  $\text{CO}_2$  and  $\text{CH}_3\text{OH}$  by the  $\text{K}_2\text{CO}_3/\text{TiO}_2$  catalyst. The computed reaction energy profile is shown in Fig. 1. Firstly, the two possible mechanisms of  $\text{C}_6\text{H}_6$  C–H bond deprotonation were evaluated and it was found that the direct C–H carboxylation of benzene with activated  $\text{CO}_2$  is preferred over the  $\text{C}_6\text{H}_6$  deprotonation (Fig. S2 and discussion, ESI†). Therefore, we proposed that the reaction starts with the adsorption of  $\text{CO}_2$  through bidentate coordination with the interface  $\text{Ti}^{3+}$  and  $\text{K}^+$  sites. The presence of  $\text{K}_2\text{CO}_3$  prevents a bidentate adsorption mode of  $\text{CO}_2$  with two  $\text{Ti}^{3+}$  surface atoms which occur on the bare defective  $\text{TiO}_2$  surface. In the next step, the C–C bond formation between the co-adsorbed benzene and  $\text{CO}_2$  occurs to form the  $\text{C}_6\text{H}_6\text{COO}^*$  intermediate ( $\text{C}_6\text{H}_6\text{CO}_2^* \rightarrow \text{C}_6\text{H}_6\text{COO}^*$ ). This step is endothermic with  $\Delta E = 0.46$  eV and it proceeds with an activation energy ( $E^\ddagger$ ) of 0.72 eV. Next, the C–H bond of the activated  $\text{C}_6\text{H}_6$  fragment is cleaved to form benzoic acid ( $\text{C}_6\text{H}_5\text{COOH}^*$ ) or benzoate ( $\text{C}_6\text{H}_5\text{COO}^*$ ) surface intermediate. The former is formed via a direct intramolecular H-transfer from the  $\text{C}_6\text{H}_6$  moiety of  $\text{C}_6\text{H}_6\text{COO}^*$  to terminal O of the carboxylate moiety. The computed activation barrier for this step is 1.31 eV. An alternative path involves a two-step surface-assisted H\*-transfer, upon which the  $\text{C}_6\text{H}_6\text{COO}^*$  intermediate is first deprotonated by the vicinal basic surface O sites ( $E^\ddagger = 1.19$  eV) followed by the  $\text{C}_6\text{H}_5\text{COO}^*$  and  $\text{H}^*$  recombination ( $E^\ddagger = 1.19$  eV). The highest activation energy of the indirect route is only ca. 0.10 eV lower than that of the direct pathway, indicating that both reaction routes can contribute to the

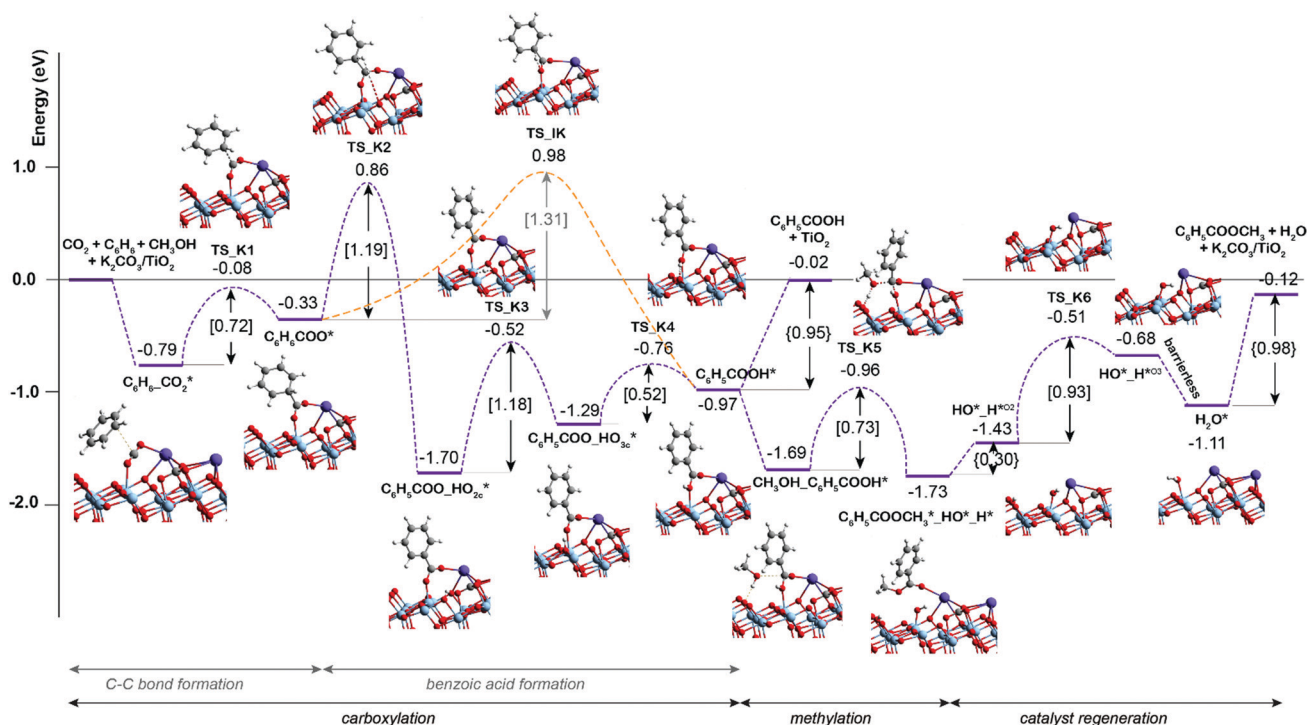


**Fig. 1** DFT-computed reaction energy diagram for the benzene esterification with  $\text{CO}_2$  and  $\text{CH}_3\text{OH}$  on  $\text{K}_2\text{CO}_3/\text{TiO}_2$ .



catalytic reaction. The hydrogen transfer from the  $C_6H_6COO^*$  to form  $C_6H_5COO^*$  is predicted to be more difficult than the initial coupling of  $CO_2$  and benzene, which is consistent with the experimentally observed kinetic isotopic effect results.<sup>9</sup> Electronic analysis further indicated that effective charge transfer between intermediates and the defective catalyst surface facilitates the C–C coupling and deprotonation reaction processes (Fig. S3 and S4, ESI<sup>†</sup>). The desorption of benzoic acid to regenerate the catalytic interface is endothermic by 0.95 eV.

The closure of the catalytic cycle can be facilitated in the presence of methanol, which reacts with the surface benzoate intermediate ( $CH_3OH\_C_6H_5COOH^*$ ) to produce methyl benzoate product ( $C_6H_5COOCH_3\_HO\_H^*$ ). During the methylation process, a  $CH_3OH$  molecule is added to the system and co-adsorbed at the neighboring surface oxygen atom of benzoic acid. Then, the methyl benzoate is generated by the formation of the C–O bond between  $CH_3OH$  and benzoic acid. The simultaneous deprotonation of  $CH_3OH^*$  and cleavage of the C–OH bond of  $C_6H_5COOH^*$  result in the generation of two hydroxyl groups on the surface. This concerted step is slightly exothermic and proceeds with an activation energy of 0.73 eV. In the next step, the methyl benzoate product is desorbed from the surface with  $\Delta E$  of 0.30 eV. The last step is the recombination of surface OH groups to form  $H_2O$  and regenerate the catalytic interface sites ( $HO^*\_H^*O_2 \rightarrow H_2O^*$ ). This dehydration step is barrierless but proceeds with a barrier of 1.00 eV associated with the surface migration of  $H^*$ . The hydrogen transfer step following the C–C bond formation is identified as

the most difficult step of the carboxylation reaction having the highest activation barrier of 1.31 eV along the reaction path.

Previous experimental studies<sup>9</sup> showed that the carbonate-free defective  $TiO_2$  can also promote benzene carboxylation but it loses the activity already after the first reaction cycle. We therefore hypothesized that the reaction intermediates or the reaction products (*e.g.* methyl benzoate or water) might block the active site of the bare  $TiO_2$  catalyst, while the presence of  $K_2CO_3$  species protects catalyst from such poisoning. To check this hypothesis, the DFT analysis was extended to the mechanism of benzene carboxylation followed by methylation on the bare and defective anatase  $TiO_2$  (101) surface. Fig. 2 presents the respective DFT-computed reaction energy diagram. In this case, the C–C bond formation between  $CO_2$  and benzene is thermodynamically and kinetically more favorable than on the interface site ( $\Delta E = -0.63$  eV,  $E^\ddagger = 0.12$  eV). However, the subsequent  $H^*$  transfer to directly form adsorbed benzoic acid is in this case 0.3 eV higher than over the  $K_2CO_3/TiO_2$ . A much more favorable reaction is the benzoate formation *via* the hydroxylation of the  $TiO_2$  surface. This step has a barrier of 1.1 eV and stabilizes the system by  $\Delta E$  of  $-1.3$  eV. Almost identical energetics was observed for the  $K_2CO_3/TiO_2$  catalyst. For the subsequent concerted benzoic acid methylation reaction, the activation energy over defective  $TiO_2$  is 0.36 eV higher than that of  $K_2CO_3/TiO_2$  catalyst reaction ( $TS\_B5 = 1.09$  eV *vs.*  $TS\_K5 = 0.73$  eV).

The comparison of the reaction profiles in Fig. 1 and 2 reveals that the activation energies of all elementary steps

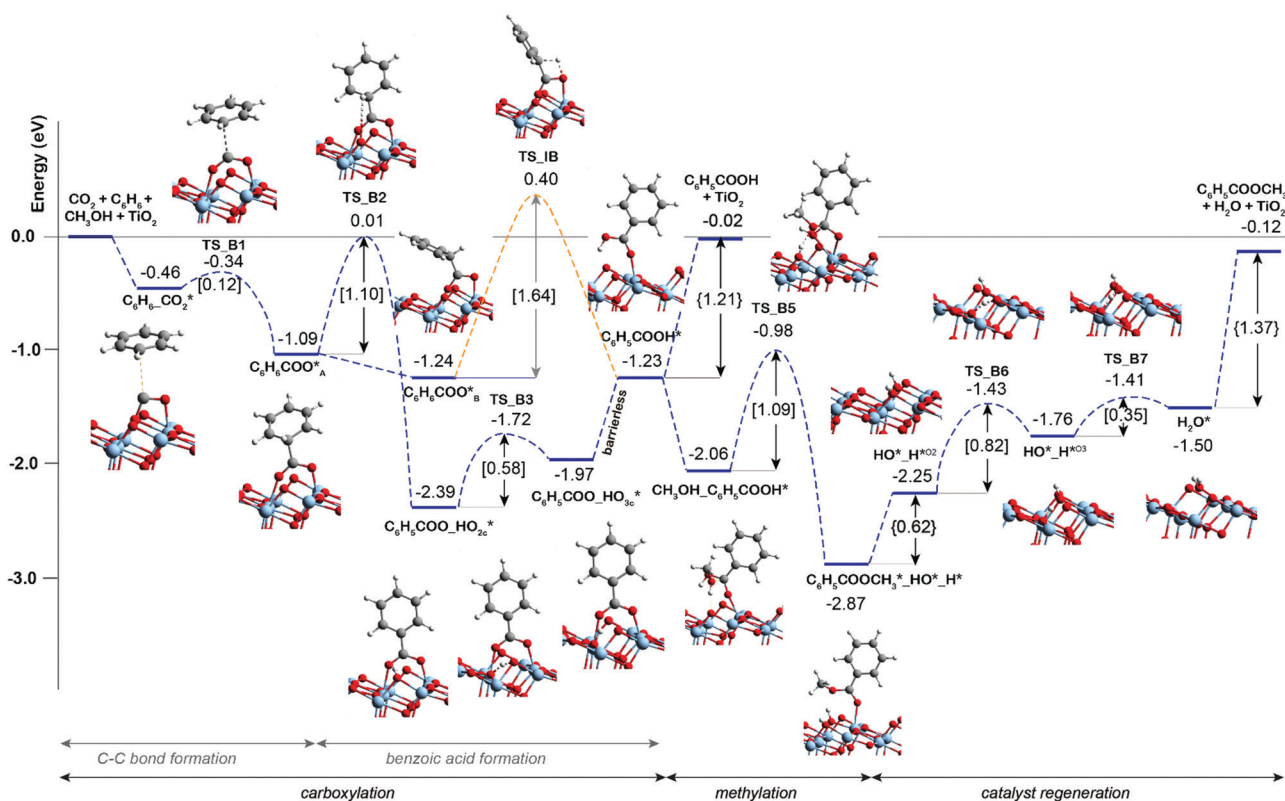


Fig. 2 Reaction energy diagram for the benzene esterification with  $CO_2$  and  $CH_3OH$  on defective  $TiO_2$  surface.



(except the initial CO<sub>2</sub> coupling with benzene) over the defective TiO<sub>2</sub> surface and K<sub>2</sub>CO<sub>3</sub>-promoted TiO<sub>2</sub> are quite close and comparable suggesting that indeed both catalysts can enable the esterification reaction of benzene with CO<sub>2</sub> and CH<sub>3</sub>OH to form methyl benzoate. However, we find that most of the reaction intermediates on the defective TiO<sub>2</sub> surface are significantly more stable than those on K<sub>2</sub>CO<sub>3</sub>/TiO<sub>2</sub>. The energies of all reaction intermediates on the defective TiO<sub>2</sub> surface are in the range of 0.00 to −3.00 eV, while those on K<sub>2</sub>CO<sub>3</sub>/TiO<sub>2</sub> catalyst fall in the range of +1.00 to −2.00 eV relative to the reactant state. The stronger binding interaction on the bare TiO<sub>2</sub> surface impedes the desorption of the products and regeneration of the active site for the next catalytic cycle (Fig. S5, ESI†). Specifically, the desorption energies of methyl benzoate and H<sub>2</sub>O on the defective TiO<sub>2</sub> surface are 0.39 and 0.32 eV higher than that on K<sub>2</sub>CO<sub>3</sub>/TiO<sub>2</sub>, respectively ( $\Delta E_{\text{C}_6\text{H}_5\text{COOCH}_3}$ : 1.37 eV vs. 0.98 eV;  $\Delta E_{\text{H}_2\text{O}}$ : 0.62 eV vs. 0.30 eV).

Based on these results, we conclude that both bare TiO<sub>2</sub> with oxygen vacancy and K<sub>2</sub>CO<sub>3</sub>/TiO<sub>2</sub> catalysts are able to activate CO<sub>2</sub> and benzene to form benzoate products. However, the excessive reactivity of the surface sites in the former results in surface poisoning by the reaction products/byproducts. The presence of potassium carbonate species partially deactivates the reactive sites on the titanium surface to facilitate the product desorption and the regeneration of the catalytic interface sites. Although the K<sub>2</sub>CO<sub>3</sub> species cannot act as an active site alone for this reaction, it steers the local structures of the transition states and reaction intermediates, and thus facilitates the products desorption and catalyst regeneration. These insights shed light onto the role of multicomponent reaction environments on the catalytic surface for the efficient CO<sub>2</sub> valorization and they can form a base for further development of efficient and stable catalysts for the direct carboxylation with CO<sub>2</sub> of other more challenging hydrocarbon substrates such as ethane, methane and ethylene.

Authors acknowledge financial support from the European Research Council (ERC) under the European Union's Horizon 2020 research and innovation programme (grant agreement No. 725686) J. M. gratefully acknowledges the Royal Thai Government Scholarships for the financial support. The use of supercomputer facilities was sponsored by NWO Domain Science.

## Conflicts of interest

The authors declare no conflicts of interest.

## Notes and references

- 1 M. D. Burkart, N. Hazari, C. L. Tway and E. L. Zeitler, *ACS Catal.*, 2019, **9**, 7937–7956.
- 2 A. D. N. Kamkeng, M. Wang, J. Hu, W. Du and F. Qian, *Chem. Eng. J.*, 2021, **409**, 128138.
- 3 C. Hepburn, E. Adlen, J. Beddington, E. A. Carter, S. Fuss, N. Mac Dowell, J. C. Minx, P. Smith and C. K. Williams, *Nature*, 2019, **575**, 87–97.
- 4 G. A. Olah, B. Török, J. P. Joschek, I. Bucci, P. M. Esteves, G. Rasul and G. K. Surya Prakash, *J. Am. Chem. Soc.*, 2002, **124**, 11379–11391.
- 5 A. S. Lindsey and H. Jeskey, *Chem. Rev.*, 1957, **57**, 583–620.
- 6 J. Luo, S. Preciado, P. Xie and I. Larrosa, *Chem. – Eur. J.*, 2016, **22**, 6798–6802.
- 7 K. Nemoto, H. Yoshida, N. Egusa, N. Morohashi and T. Hattori, *J. Org. Chem.*, 2010, **75**, 7855–7862.
- 8 J. Luo and I. Larrosa, *ChemSusChem*, 2017, **10**, 3317–3332.
- 9 D. J. Xiao, E. D. Chant, A. D. Frankhouser, Y. Chen, A. Yau, N. M. Washton and M. W. Kanan, *Nat. Chem.*, 2019, **11**, 940–947.
- 10 G. F. Kresse and J. Furthmüller, *Comput. Mater. Sci.*, 1996, **6**, 15–50.
- 11 G. F. Kresse and J. Furthmüller, *Phys. Rev. B: Condens. Matter Mater. Phys.*, 1996, **54**, 11169–11186.
- 12 J. P. B. Perdew, K. Burke and M. Ernzerhof, *Phys. Rev. Lett.*, 1996, **77**, 3865–3868.
- 13 G. S. Stefan, E. Stephan and G. Lars, *J. Comput. Chem.*, 2011, **32**, 1456–1465.
- 14 W. Song, S. Ma, L. Wang, J. Liu and Z. Zhao, *ChemCatChem*, 2017, **9**, 4340–4344.
- 15 D. C. Sorescu, W. A. Al-Saidi and K. D. Jordan, *J. Chem. Phys.*, 2011, **135**, 124701.

